Analytical representation for the numerical ephemeris of Titan within short time spans

X. J. Xi, A. Vienne

A&A 666, A25 (2022)
https://doi.org/10.1051/0004-6361/202243036

Astronomy & Astrophysics

Analytical representation for the numerical ephemeris of Titan within short time spans

X. J. Xi[1] and A. Vienne[2,3]

[1] National Time Service Centre (NTSC), Chinese Academy of Sciences, PO Box 18, Lintong, Shaanxi 710600, PR China
e-mail: xxj@ntsc.ac.cn
[2] IMCCE, Observatoire de Paris, PSL Research University, CNRS, Sorbonne Université, Université de Lille, 75014 Paris, France
e-mail: alain.vienne@univ-lille.fr
[3] Université de Lille, Observatoire de Lille, 59000 Lille, France

Received 4 January 2022 / Accepted 7 July 2022

ABSTRACT

Context. Numerical integration ephemerides are widely used in research and engineering for their high precision. However, subject to their finite available time spans, their use is limited in theoretical research, such as the studies of rotation and evolution. Previously, we successfully experimented on the analytical representation of the mean longitude of Titan of the Jet Propulsion Laboratory (JPL) ephemeris, as a function of combinations of proper frequencies, and related the results with what is given in the synthetic ephemerides obtained by the Théorie Analytique des Satellites de Saturne (TASS).
Aims. In this study, the analytical representations of the other osculating elements of the JPL Titan ephemeris are accomplished in order to construct the new synthetic representations, which have the advantages of both systems: long-lasting stability, the system details of TASS, and the high precision of JPL.
Methods. A frequency analysis process was used to obtain the proper frequencies, amplitudes, and phases of the two ephemerides in the short term and the semi-long terms. For the proper frequency of the ascending node of Titan, which has a very long period, it is challenging to acquire the exact value, and the formula of TASS was used. The amplitude and phase of long terms were further calculated by a least-squares procedure.
Results. Thanks to the accomplishments of the new synthetic representations of the JPL ephemeris, we report the complete combinations of the osculating elements of Titan. These combinations contain important dynamical information such as the proper frequencies. They will be useful in the theoretical research.

Key words. ephemerides – celestial mechanics – methods: numerical – methods: analytical – planets and satellites: individual: Titan

1. Introduction

The numerical integration ephemerides of natural satellites are widely used for their high precision. However, this advantage does not promote their use in the scientific studies of rotation and evolution as their finite time spans place serious restrictions on obtaining the motion details from the ephemerides. We work to represent the numerical integration ephemerides in the form of combinations of related proper frequencies, called the analytical representation, which have the advantages of long-lasting stability and high precision. This representation explicitly describes the motion details of the planet system.

In our previous work (Xi & Vienne 2020; hereafter Paper I), we successfully obtained the representation of the mean longitude of the JPL Titan ephemeris (Giorgini et al. 1996). Meanwhile, we obtained the proper frequencies involved using TASS as a template (Vienne & Duriez 1995). The representation included the mean motion, the constant term, and the amplitudes and phases of eight periodic and quasi-periodic terms. The mean residuals between JPL and our representation was about –13.27 m, and the standard deviation was about 26 km. Encouraged by these satisfactory results, we extend our study to the other orbital elements of Titan.

As in Paper I, here we take the TASS ephemerides as a template to successfully demonstrate how to obtain the representations of the JPL Titan ephemerides. We work on the analytical representations of the other five orbital elements: the eccentricity and the pericentre $z_6 : e_6 \cdot \mathrm{e}^{\sqrt{-1}\varpi_6}$; the inclination and the ascending node $\zeta_6 : \sin\frac{i_6}{2} \cdot \mathrm{e}^{\sqrt{-1}\Omega_6}$; and the semi-major axis a_6. The elements z_6 and ζ_6 are complex, hence each corresponds to two elements.

In Sect. 2, we give some important additional information on the JPL ephemerides and the update in early 2020. In Sect. 3, we report the short terms and semi-long terms of ζ_6 and z_6 by frequency analysis. They are later removed to simplify the calculation.

A nominal value of the proper frequency for the ascending node of Titan Ω_6^*, according to a TASS formula, is adopted from Paper I. This nominal value plays an important role in the analytical representation of ζ_6 in this study. The discussion related to ζ_6 is presented in Sect. 4.

Our experience with ζ_6 promotes us to further analyse the residuals in order to find the additional short-term components. These terms usually have very small amplitudes, one or two orders of magnitude less than the major ones. Thus, they exist but are hidden in the residuals. The representation of z_6 is displayed in Sect. 5.

The representation of the semi-major axis a_6 (Sect. 6), which involves numerous short-period terms, and the updated mean

longitude λ_6 (Sect. 7) are conducted in this study. The latter now has 15 instead of 8 components, as well as a smaller standard deviation.

Put together, we can report the representations of all the elliptic elements of Titan (Sect. 8). The representations have almost the same precision as the original Titan ephemeris of JPL with the same time duration. However, the dynamic information that they contain can be used over a much longer time period. All the derived equations used in the study are listed in the Appendix. A more detailed description of the synthetic representation of the motion can be found in Paper I.

2. Ephemerides information

It is necessary to mention some information on the ephemerides. As was done in Paper I, each orbit of the satellites in this study is described by the osculating elements p, λ, z, and ζ, following the work of Duriez (Duriez 1979, 1977):

$$\begin{aligned} a &= A(1+p)^{-2/3} \Longleftrightarrow n = N(1+p),\\ \lambda &= Nt + \lambda_0 + r,\\ z &= e\exp\sqrt{-1}\varpi,\\ \zeta &= \sin\frac{i}{2}\exp\sqrt{-1}\Omega. \end{aligned} \tag{1}$$

The JPL ephemerides are presented in either the classical elliptic element form as $(a, e, i, \omega, \varpi, M)$ or the position–velocity form in the ecliptic plane. The quantity μ in Kepler's third law $n^2a^3 = \mu$ used in this study is

$$\mu = 1.129767089077 \times 10^{-2}(\mathrm{au}^3\,\mathrm{y}^{-2}). \tag{2}$$

Here, au means astronomical units and y is year.

All motions refer to the Saturnicentric ring plane in which the origin corresponds to the node with the mean ecliptic J2000. The node and the inclination refer to the equinox and ecliptic J2000 system and are then defined as

$$\begin{aligned} \Omega_\mathrm{a} &= 169.5291^\circ,\\ i_\mathrm{a} &= 28.0512^\circ. \end{aligned} \tag{3}$$

The orbital elements of JPL are transformed into the same form as (a, λ, z, ζ) on the Saturn ring plane with Eqs. (2) and (3).

An update was made by JPL to the ephemerides of its Saturnian satellites in early 2020 based on the final Cassini comprehensive reconstruction. However, the available time span of the new version is about 500 yr, which does meet our computation requirements. In this research we use the same ephemeris of Titan as in Paper I, which was first published in 2016 with an official accuracy of 10 km. The corresponding ephemeris is available upon request. All the physical parameters of the Solar System were downloaded from the JPL official website in 2019.

For simplicity, we abbreviate some of the repeated concepts in this study. We refer to the TASS template as TASS-t (see Paper I), which corresponds to the representations of all the orbital elements of TASS, with all the proper frequencies of the Saturn system. Similarly, XA-JPL represents all the parameters, proper frequencies, and representations of the JPL ephemerides. FA is the abbreviation for frequency analysis, and LSM for the least-squares method.

The proper frequencies related to the representations are the following:

Table 1. Values of the proper frequencies of TASS and JPL.

ID	TASS-t (radian year^{-1})	XA-JPL (radian year^{-1})
λ_2^*	1674.867298497696	1674.862700502130
λ_3^*	1215.663929056177	1215.662981284389
λ_4^*	838.510870359548	838.522569478004
λ_6^*	143.924047849167	143.924045534754
λ_5^*	508.009320172829	508.009309199013
ϖ_6^*	0.008933864296	0.008922847882
ϖ_8^*	0.001974690829	0.001974690829
Ω_5^*	−0.175467623487	−0.175359995366
Ω_6^*	−0.008931239595	0.008935057595
Ω_8^*	−0.001925543593	−0.001925543593
λ_s^*	0.213382895534	0.213342329926
λ_J^*	0.529690977758	0.529673420072
Λ_6	0.006867993783	0.006867993783
ω_6	3.583299718564	**

λ_2^* the mean longitude of Enceladus;
λ_3^* the mean longitude of Tethys;
λ_4^* the mean longitude of Dione;
λ_5^* the mean longitude of Rhea;
λ_6^* the mean longitude of Titan;
λ_s^* the mean longitude of the Sun;
ϖ_6^* the pericentre of Titan;
ϖ_8^* the pericentre of Iapetus;
Ω_5^* the ascending node of Rhea;
Ω_6^* the ascending node of Titan;
Ω_8^* the ascending node of Iapetus;
Λ_6 an undefined frequency used in TASS;
ω_6 the libration argument of the Titan-Hyperion resonance.

The proper frequencies of TASS and JPL relative to this work can be found in Table 1. The superscript asterisk (*) indicates a corresponding argument to the proper frequencies. Proper frequencies are the physical characteristics, thus their values remain constant throughout the corresponding dynamical system. However, readers can find small differences in their values between Table 1 and the other tables. For example, we see the different values of λ_s in Table 1, Table 7, and Table 11. The value of λ_s in Table 7 and Table 11 are thought to be influenced by some long-period perturbations. However, the perturbation changes too slowly to be identified, for instance about 10^{-4} radian per year in Table 7. Therefore, we represent this component just as λ_s and ignore the perturbation.

The argument ω_6 is associated with the 3:4 resonance relation between Titan and Hyperion, which leads to a libration of the angle $3\lambda_6 - 4\lambda_7 + \varpi_7^*$. We can use ω_6 to take the place of ϖ_7^*. More details on this can be found in Vienne & Duriez (1991). The lack of this resonance argument limits us to obtain the value of ω_6 from JPL. The TASS-t value is used in this work.

The osculating elements can be documented as the sum of finite integer combinations of the proper frequencies. Similar components between different ephemerides are compared repeatedly. To make the comparisons more intuitive and understandable, we change the units of amplitudes from radians to kilometres, by multiplying the corresponding amplitudes by the mean value of the semi-major axis of Titan, 1221870.0 km.

More details on the synthetic representation of motion can be found in Paper I, and is not further discussed here. We report the equations of our method in the Appendix.

Table 2. Short terms and semi-long terms of z_6 in JPL.

ID	Frequency (radian year^{-1})	Amplitude (km)	Phase (radian)
$2\lambda_s^* - \varpi_6^*$	0.417768526306	91.50	−0.73810267
λ_6^*	143.924045533325	81.89	−0.56569307
λ_5^*	508.009309191022	11.38	0.21320802
$3\lambda_s^* - \varpi_6^*$	0.631043871764	11.57	−1.48047273

Table 3. Short terms and semi-long terms of ζ_6 in JPL.

ID	Frequency (radian year^{-1})	Amplitude (km)	Phase (radian)
$2\lambda_s^*$	0.426696791114	138.74	2.04928518
$-\lambda_s^*$	−0.213245071964	23.70	0.80734540
$3\lambda_s^*$	0.639979694841	17.88	1.30707517
λ_s^*	0.213248348339	14.47	2.30454997

3. Determination of the short terms and semi-long terms

The short terms and semi-long terms are predetermined by TASS-t combinations, and are obtained by frequency analysis. These terms are removed later to simplify the subsequent calculations. They are given in Table 2 for z_6 and in Table 3 for ζ_6.

After removing the components motioned above, we used the LSM to determine the amplitude and phase of the long terms. The short terms and semi-long terms of the two ephemerides are not exactly the same, especially those with amplitudes of less than 10 km. We list all the obtained short terms and semi-long terms of ζ_6 and z_6 in Sects. 4 and 5.

4. Representation of the inclination and ascending node of Titan ζ_6 of JPL

In TASS-t, there is a constant-like component with null frequency. However, the finite time span of JPL limits us to distinguishing this term from the major period term, which is associated with the ascending node Ω_6. Unfortunately, the LSM cannot make the differentiation. The difference in the constant-like component value between TASS-t and the LSM over the same time span (10 000 yr) is important, about 165.1 km, which is much greater than the 20 km difference in ζ_6 between JPL and TASS at the J2000.0 epoch.

Similarly, the obtained value of 1000 yr for TASS is also not acceptable. Therefore, we chose the TASS-t value for the constant-like component of JPL. The results are reported in Table 4.

In Paper I, we use a nominal value for the proper frequency of the ascending node of Titan Ω_6. It works well in the representation of the mean longitude. A proper frequency as the physical characteristic should remain constant throughout the system. We bring separately the nominal value and the TASS-t value in the calculations of the representation of ζ_6 in order to verify the correction and its wide application.

We report the comparison of presentations between TASS and JPL in Table 5. The solution of the four major terms, for which the TASS-t value of Ω_6^* is adopted, is listed in Table 6.

Table 4. Value of constant-like component in ζ_6 in different time spans of TASS.

(radian)	Time span (years)	Method
−0.005583725984	10 000	FA
−0.005448610014	10 000	LSM
−0.005793205614	1000	LSM

Table 5. Comparison of the solutions of ζ_6 between TASS and XA-JPL.

ID	Frequency (radian year^{-1})	Amplitude (radian)	(km)	Phase (radian)	
	−0.000000000000	0.0056023641	**	−3.06168702	TASS-t
Ω_6^*					
	−0.008931239594	0.0027899429	3408.95	−0.25711520	TASS-t
	−0.008935057595	0.0027364047	3343.53	−0.27676016	XA-JPL
Ω_8^*					
	−0.001925543576	0.0001312363	160.35	−1.27742697	TASS-t
	−0.001925543593	0.0002822330	344.85	−0.32079820	XA-JPL
$2\Omega_8^*$					
	−0.003851087191	0.0000094698	11.57	−2.63456161	TASS-t
	−0.003851087186	0.0000387493	47.35	2.27501684	XA-JPL
$2\lambda_J^* - 5\lambda_s^*$					
	−0.006831187831	0.0000110589	13.51	−2.60258392	TASS-t
$2 \times (2\lambda_J^* - 5\lambda_s^*)$					
	−0.014731799789	0.0000076539	9.35	2.83771472	XA-JPL
$-\Omega_8^* + \Upsilon$					
	0.002172687403	0.0001672175	204.32	−2.78725535	XA-JPL
$2\lambda_s^*$					
	0.426598241223	0.0001125670	137.54	2.04979896	TASS-t
	0.426696791114	0.0001137550	138.99	2.04928518	XA-JPL
$-\lambda_s^*$					
	−0.213299120064	0.0000191667	23.42	0.82899234	TASS-t
	−0.213245071964	0.0000193978	23.70	0.80734540	XA-JPL
$3\lambda_s^*$					
	0.639897360235	0.0000149794	18.30	1.30207992	TASS-t
	0.639979694841	0.0000146349	17.88	1.30707517	XA-JPL
λ_s^*					
	0.213299120067	0.0000114462	13.99	2.28081791	TASS-t
	0.213248348339	0.0000118455	14.47	2.30454997	XA-JPL

The first part of Table 5 shows the long terms relative to the representation of ζ_6, labelled XA-JPL, and the related TASS-t terms. They are Ω_6^*, Ω_8^*, $2\Omega_8^*$, and $2\lambda_J^* - 5\lambda_s^*$. There is a slight difference in component values in $2\lambda_J^* - 5\lambda_s^*$ and $4\lambda_J^* - 10\lambda_s^*$ when comparing TASS and XA-JPL. The representation of JPL in Table 5 is the solution of the nominal value.

Likewise, we list the solution of ζ_6 in Table 6, for which the TASS-t value of Ω_6^* is adopted. A small difference between Ω_6^* in TASS-t and JPL makes no influence on the solution of Ω_6^* itself. It clearly only affects the solutions of the long terms Ω_8^*, $2\Omega_8^*$, and $2 \times (2\lambda_J^* - 5\lambda_s^*)$. In addition, it interferes with the value $-\Omega_8^* + \Upsilon$, listed in the second part of Table 5. Its frequency is closed to Ω_8^*, which is considered a combination of $-\Omega_8^*$ and a very long period perturbation Υ (about 1 Myr). Its amplitude is about 205 km. It is the third huge term of the representation of ζ_6. The absence of this term brings a misfit and causes the residuals between this solution and JPL to increase with time, as we see in Fig. 1.

Finally, we obtain the representation of the inclination and ascending node ζ_6 for JPL. The mean of the residuals between

Table 6. Solutions of ζ_6, with Ω_6^* of TASS-t.

ID	Frequency (radian year^{-1})	Amplitude (radian)	(km)	Phase (radian)
Ω_6^*				
	−0.008693210604	0.0027079315	3347.68	−0.29529223
Ω_8^*				
	−0.001925543593	0.0001535753	192.42	0.24761346
$2\Omega_8^*$				
	−0.003425316835	0.0001294861	158.22	2.64543722
$2\times(2\lambda_J^*-5\lambda_s^*)$				
	−0.013799613776	0.0000877907	107.30	0.15295797

Table 7. Inclination and ascending node of Titan from JPL in the form $\zeta_6 = \sum_{i=1}^{n_t} A_i \cos(\omega_i t + \phi_i) + \imath \times \sum_{i=1}^{n_t} A_i \sin(\omega_i t + \phi_i)$.

n°	Frequency (radian year^{-1})	Amplitude (radian)	(km)	Phase (radian)	ID
	−0.000000000000	0.0056023641		−3.06168702	
1	−0.008935057595	0.0027364047	3343.53	−0.27676016	Ω_6^*
2	−0.001925543593	0.0002822330	344.85	−0.32079820	Ω_8^*
3	0.002172687403	0.0001672175	204.32	−2.78725535	$-\Omega_8^*+\Omega$
4	0.426696791114	0.0001137550	138.99	2.04928518	$2\lambda_s^*$
5	−0.003851087186	0.0000387493	47.35	2.27501684	$2\Omega_8^*$
6	−0.213245071964	0.0000193978	23.70	0.80734540	$-\lambda_s^*$
7	0.639979694841	0.0000146349	17.88	1.30707517	$3\lambda_s^*$
8	0.213248348339	0.0000118455	14.47	2.30454997	λ_s^*
9	0.010884230625	0.0000080643	9.85	0.11060790	$\varpi_6^*-\Omega_8^*$
10	−0.014731799789	0.0000076539	9.35	2.83771472	$4\lambda_J^*-10\lambda_s^*$
11	−0.426738184583	0.0000056202	6.87	−1.93783340	$-2\lambda_s^*$
12	−0.019169988641	0.0000024381	2.98	0.00180791	$-2\varpi_6^*-2\Omega_8^*$
13	−0.175339675092	0.0000021008	2.57	2.27751400	Ω_5^*

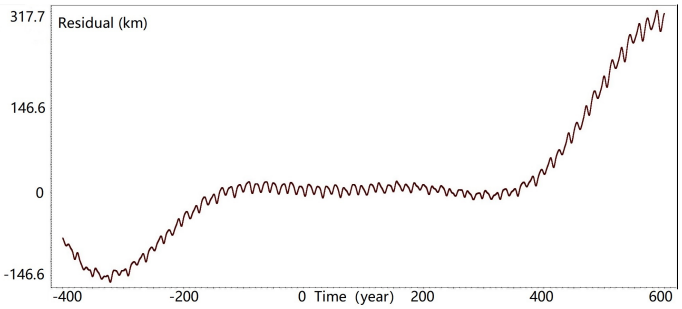

Fig. 1. Residuals of ζ_6 between the solution of TASS-t Ω_6^* and JPL.

the XA-JPL and JPL ephemeris is about 360.97 m, and the standard deviation is about 5.76 km.

5. JPL representation of the eccentricity and the pericentre of Titan z_6

The calculation for z_6, the eccentricity and pericentre of Titan, is simpler than that of ζ_6. The involved proper frequencies are more accurate. As in the previous section, we remove the short terms and semi-long terms first, and then we determine their long terms by a simplified LSM. The solution is listed in Table 9. The mean of the residuals between XA-JPL and JPL is about −213.89 m, and the standard deviation is about 3.53 km.

A comparison between TASS-t and XA-JPL is shown in Table 8. The biggest difference comes from the major term, the pericentre of Titan ϖ_6^*, of about 86 km in the amplitude. The other differences are smaller than 10 km. XA-JPL is very close to TASS on the eccentricity and pericentre z_6.

6. JPL representation of the semi-major axis a_6 of Titan

The representation of the semi-major axis a_6 is directly obtained by frequency analysis. The main components of a_6 in TASS and JPL are similar. XA-JPL has numerous small-amplitude short terms, whose amplitudes reach several hundred metres. The representation of the semi-major axis is listed in Table 10.

7. Updated JPL representation of the mean longitude λ_6 of Titan

An update of the mean longitude λ_6 is calculated, inspired by the discovery of new small-amplitude short terms listed above. Its components have increased from 8 to 15 terms, listed in Table 11; the first eight columns consist of the components reported in Paper I, and the last seven columns consist of the new terms obtained in this study.

It is noteworthy that the mean of the residuals between XA-JPL and JPL increases from −13.27 m to 35.45 m; however, the standard deviation decreases from 25.59 km to 12.47 km, compared with the results in Paper I.

8. Synthetic representation of Titan

Here, we give a complete analytical representation of all the osculating elements of Titan from JPL: a_6 is the semi-major axis in Table 10; λ_6 is the mean longitude in Table 11; z_6 is the eccentricity and the pericentre in Table 9; and ζ_6 is the inclination and the ascending node in Table 7. The representations of Titan are composed of all these tables, and are named XA-JPL. The corresponding software to compute the orbital elements with these tables is available on request. The software also can calculate the orbit in the form of position-velocities referring to the equinox and ecliptic J2000 system with Eqs. (2) and (3).

9. Conclusions

In this work, we established a connection between the theoretical ephemerides and the numerical integration ephemerides. We completed the analytical representations of the osculating elements of the JPL Titan ephemeris and obtained most of the proper frequencies related to the representations, consisting of all the major proper frequencies of Titan, including the mean longitude and the ascending node of Rhea and the mean longitude of Enceladus, Tethys, Dione, and Iapetus.

Our representations report the system dynamic information and the detailed perturbation relationship of JPL, which were not clearly exhibited before. The standard deviation between XA-JPL and JPL in position is smaller than 628.19 m, and the mean residual is only several centimetres.

We expect to make further research on the representations of other major Saturn satellites, to get more proper frequencies and dynamic information on the Saturn system. Moreover, we would like to make a similar study on other Saturnian numerical ephemerides like NOE (Lainey et al. 2004a,b), and also on the numerical ephemerides of the satellites of other planet systems, such as the Martian satellites.

Table 8. Comparison of the solutions of z_6 between TASS and XA-JPL.

ID	Frequency (radian year^{-1})	Amplitude (radian)	(km)	Phase (radian)	EPH
ϖ_6^*					
	0.008933864289	0.0289265365	35344.467153	2.86627922	TASS-t
	0.008922847865	0.0288561951	35258.519153	2.86729807	XA-JPL
$-\varpi_6^*$					
	−0.008933959907	0.0001921234	234.749826	0.42638138	TASS-t
	−0.008922847882	0.0001919517	234.539964	0.45372682	XA-JPL
$\varpi_6^* + \Omega_8^*$					
	0.007008286694	0.0000242939	29.683988	−1.64598798	TASS-t
	0.006997304289	0.0000295358	36.088945	−0.08850508	XA-JPL
$\varpi_6^* - \Omega_8^*$					
	0.010859401773	0.0000239166	29.222976	−2.06132503	TASS-t
	0.010848391475	0.0000189882	23.201104	2.55593623	XA-JPL
ϖ_8^*					
	0.001974774505	0.0000172066	21.024228	−2.82136616	TASS-t
	0.001974690829	0.0000239209	29.228280	−2.66393868	XA-JPL
$-\varpi_6^* + 2\lambda_s^*$					
	0.417664365570	0.0000744656	90.987283	−0.72852474	TASS-t
	0.417768526921	0.0000747215	91.299928	−0.73810273	XA-JPL
λ_6^*					
	143.924047290026	0.0000668787	81.717077	−0.56432198	TASS-t
	143.924045533834	0.0000670170	81.886073	−0.56569312	XA-JPL
λ_5^*					
	508.009320171889	0.0000101008	12.341865	0.21391389	TASS-t
	508.009309191028	0.0000093102	11.375878	0.21320802	XA-JPL
$-\varpi_6^* + 3\lambda_s^*$					
	0.630963495932	0.0000096035	11.734229	−1.47873726	TASS-t
	0.631043870540	0.0000094202	11.510243	−1.48047261	XA-JPL

Table 9. Eccentricity and pericentre of Titan from JPL in the form $z_6 = \sum_{i=1}^{n_t} A_i \cos(\omega_i t + \phi_i) + \imath \times \sum_{i=1}^{n_t} A_i \sin(\omega_i t + \phi_i)$.

n°	Frequency (radian year^{-1})	Amplitude (radian)	(km)	Phase (radian)	ID
1	0.008922847865	0.0288561951	35258.52	2.86729807	ϖ_6^*
2	−0.008922847882	0.0001919517	234.54	0.45372682	$-\varpi_6^*$
3	0.006997304289	0.0000295358	36.09	−0.08850508	$\varpi_6^* + \Omega_8^*$
4	0.010848391475	0.0000189882	23.20	2.55593623	$\varpi_6^* - \Omega_8^*$
5	0.001974690829	0.0000239209	29.23	−2.66393868	ϖ_8^*
6	0.417768526921	0.0000747215	91.30	−0.73810273	$-\varpi_6^* + 2\lambda_s^*$
7	143.924045533834	0.0000670170	81.89	−0.56569312	λ_6^*
8	508.009309191028	0.0000093102	11.38	0.21320802	λ_5^*
9	0.631043870540	0.0000094202	11.51	−1.48047261	$-\varpi_6^* + 3\lambda_s^*$
10	0.204292533874	0.0000055655	6.80	3.10679045	$\lambda_s^* - \varpi_6^*$
11	838.510861768628	0.0000052056	6.36	2.39023743	λ_4^*
12	−220.161218121711	0.0000045462	5.55	−1.34459433	$-2\lambda_6^* - \lambda_5^*$
13	−143.497357562492	0.0000044228	5.40	2.69551544	$2\lambda_s^* - \lambda_6^*$
14	−0.325963534329	0.0000039916	4.88	0.25145162	$\lambda_s^* - \lambda_J^* - \varpi_6^*$
15	0.015381175333	0.0000035231	4.30	−2.4324747	$2\varpi_6^* + \Omega_8^*$
16	1215.663927998115	0.0000033177	4.05	2.59058838	λ_3^*
17	−0.003564170042	0.0000031913	3.90	−3.08334138	$2\Omega_8^*$
18	287.839169160205	0.0000028229	3.45	2.28446256	$2\lambda_6^* - \varpi_6^*$
19	−550.662770700905	0.0000023070	2.82	2.76156172	$-\lambda_4^* + 2\lambda_6^*$
20	−0.4177851750182	0.0000022342	2.73	−2.25592112	$-2\lambda_s^* + \varpi_6^*$
21	0.221880937275	0.0000020679	2.53	2.24080336	$\lambda_s^* + \Omega_6^*$
22	−0.204066424890	0.0000019935	2.44	0.41114421	$-\lambda_s^* + \Omega_6^*$
23	0.434415938186	0.0000018714	2.29	−1.36938699	$2\lambda_s^* + \varpi_6^*$
24	−0.020728682845	0.0000018148	2.22	0.30124005	$-2\varpi_6^* + 2\Omega_8^*$

Table 10. Semi-major axis of Titan from JPL in the form $a_6 = a_0 + \sum_{i=1}^{n} A_i \cos(\omega_i t + \phi_i)$.

	Frequency (radian year^{-1})	Amplitude (au)	(km)	Phase (radian)	ID
	0.000000000000	0.0081682112	1221947.00	0.00000000	a_0
n°	(radian year^{-1})	(au $\times 10^7$)	(km)	(radian)	
1	−364.085263656371581	1.28608880	19.24	−0.77890118	$\lambda_6^* - \lambda_5^*$
2	694.586816233811760	0.66298636	9.92	2.95593059	$\lambda_4^* - \lambda_6^*$
3	−1071.739882463474714	0.40390842	6.04	3.12690378	$\lambda_6^* - \lambda_3^*$
4	143.915125188810634	0.31540302	4.72	2.85003567	$\lambda_6^* - \varpi_6^*$
5	−287.421403131497300	0.24036750	3.60	−3.02198337	$-2\lambda_6^* + 2\lambda_s^*$
6	1530.943223018746039	0.07645178	1.14	3.04920192	$\lambda_2^* - \lambda_6^*$
7	287.208108160346001	0.04627154	0.69	−2.51550026	$2\lambda_6^* - 3\lambda_s^*$
8	−220.170140158743123	0.04333216	0.65	2.07124940	$2\lambda_6^* - \lambda_5^*$
9	−728.170527313752359	0.03976144	0.59	1.58379043	$-2\lambda_5^* - 2\lambda_6^*$
10	−287.848139938724842	0.01345982	0.20	1.31699297	$2\lambda_6^* - \varpi_6^*$

Table 11. Mean longitude of Titan from JPL in the form $\lambda_6 = Nt + \lambda_0 + \sum_{i=1}^{n} A_i \sin(\omega_i t + \phi_i)$.

n°	Frequency (radian year^{-1})	Amplitude (radian)	(km)	Phase (radian)	ID
	143.924045534754				N
				5.718878	λ_0
1	0.001925543543	0.0015494050	1893.17	−1.745326	$-\Omega_8^*$
2	0.008935057595	0.0006308411	770.81	0.343321	$-\Omega_6^*$
3	0.426697846565	0.0002067870	252.67	−1.158157	$2\lambda_s^*$
4	0.213381048936	0.0001830009	223.60	2.420117	λ_s^*
5	0.006874219340	0.0000326175	39.85	2.437628	Λ_6
6	0.639897726868	0.0000291066	35.56	−1.918137	$3\lambda_s^*$
7	0.017845695764	0.0000273363	33.40	2.418477	$2\varpi_6^*$
8	364.085261349846	0.0000111378	13.61	0.779460	$\lambda_5^* - \lambda_6^*$
9	−3.583073740059	0.0000036207	8.85	−1.792328	ω_6
10	694.586816236757	0.0000063831	7.80	2.955931	$\lambda_4^* - \lambda_6^*$
11	143.915119280905	0.0000061830	7.55	2.850461	$\lambda_6^* - \varpi_6^*$
12	−0.436279553701	0.0000056291	6.88	2.955931	$-2\lambda_s^* - \varpi_6^*$
13	287.421403265371	0.0000051500	6.29	−0.119591	$2\lambda_6^* - 2\lambda_s^*$
14	0.718183613841	0.0000043221	5.28	2.773366	$\lambda_s^* - \lambda_J^* + 2\varpi_6^* - 2\Omega_8^*$
15	0.212813032048	0.0000015001	3.67	1.624010	$\lambda_s^* - \varpi_6^*$

Acknowledgements. We thank Melaine Saillenfest for the use of his software of frequency analysis. The authors also thank the reviewer for very useful and helpful comments. X.J. Xi acknowledges a financial support from the National Science Foundation of China (NSFC) (12173042).

References

Duriez, L. 1977, A&A, 54, 93
Duriez, L. 1979, PhD Thesis, Université de Lille, France
Giorgini, J. D., Yeomans, D. K., Chamberlin, A. B., et al. 1996, Bull. Am. Astron. Soc., 28, 1158
Jet Propulsion Laboratory (JPL) 2018, HORIZONS Web-Interface, https://ssd.jpl.nasa.gov/?horizons/
Lainey, V., Arlot, J. E., & Vienne, A. 2004a, A&A, 420, 1171
Lainey, V., Duriez, L., & Vienne, A. 2004b, A&A, 427, 371
Laskar, J. 1993, Physica D: Nonlinear Phenomena, 67, 257
Laskar, J., Froeschlé, C., & Celletti, A. 1992, Physica D: Nonlinear Phenomena, 56, 253
Saillenfest, M. 2014, Représentation synthétique du mouvement des satellites de Saturn, Report of Paris Observatory
Vienne, A. 1991, Thesis, Université de Lille, France
Vienne A., & Duriez L. 1991, A&A, 246, 619
Vienne, A., & Duriez, L. 1995, A&A, 297, 588
Xi, X, J. 2018, Thesis, Observatoire de Paris, Université PSL, France
Xi, X. J., & Vienne, A. 2020, A&A, 635, A91

Appendix A: Extension of the frequency analysis via the least-squares method

The calculation of ζ_6 or z_6 is described in this Appendix. It uses the same method for the λ_6 calculation as in Paper I. Considering an integrable Hamilton system with m degrees of freedom based on a Hamiltonian H, if the system evolves within the hypothesis of the Arnold-Liouville theorem, there are some coordinates called action-angles. The action-angle coordinates are intrinsic to the system. The first derivatives of the action variables give the proper frequencies ω_j.

When a function $f(t)$ describes a mechanical system, for example, $f(t)$ may stand for one of the variables in Eq. 2, and it can be written as a series in the form

$$f(t) = \sum_{k\in\mathbb{N}} A_k \ \exp\ i\nu_k t \text{ with } A_k \in \mathbb{C}\,, \tag{A.1}$$

where ν_j are the integer combinations of the proper frequencies ω_j.

In this paper we assume that the system is integrable, or at least close to integrable. Hence, the corresponding equation of orbital elements can be written as

$$Y(t) = \sum_{i=1}^{n_t} A_{1,i}\cos(\omega_i t + \phi_i) + \imath \times \sum_{i=1}^{n_t} A_{2,i}\sin(\omega_i t + \phi_i), \tag{A.2}$$

where $Y(t)$ is the value of ζ_6 or z_6 at time t and n_t is the number of the terms.

Each frequency ω_i can be an integer combination of several proper frequencies, a single frequency itself, or a multiple of a single frequency. The series is considered periodic or quasi-periodic. It is constructed following the D'Alembert rule (Laskar et al. 1992; Laskar 1993), where ϕ_i and A_i are the phase and amplitude related to ω_i.

In the case of the mean longitude, λ_6 has only a real part:

$$Y(t) = \sum_{i=1}^{n_t} A_{1,i} sin(\omega_i t + \phi_i). \tag{A.3}$$

The complete representation of the mean longitude needs to add its main slope Nt and initiate λ_0:

$$\lambda = Nt + \lambda_0 + \sum_{i=1}^{n_t} A_{1,i} sin(\omega_i t + \phi_i). \tag{A.4}$$

Their unknown amplitudes and phases are determined by the LSM. The semi-major axis a_6 has only a real part. It is not considered in the LSM as its representation can be obtained directly by frequency analysis.

With a step of 0.6 days over 1000 year, we have $m = 607800$ equations for each osculating element of Titan. If we use

$$\begin{cases} \sin(\omega_1 t_i) = X_{i,1} \\ \cos(\omega_1 t_i) = X_{i,2} \\ \sin(\omega_2 t_i) = X_{i,3} \\ \qquad\qquad \cdots \\ \cos(\omega_n t_i) = X_{n,n} \end{cases} \tag{A.5}$$

$$\begin{cases} a_{1,1} = A_1 \sin\phi_1 \\ a_{2,1} = A_1 \cos\phi_1 \\ a_{1,2} = A_1 \cos\phi_1 \\ a_{2,2} = -A_1 \sin\phi_1 \\ a_{1,3} = A_2 \sin\phi_2 \\ a_{2,3} = A_2 \cos\phi_2 \\ a_{1,4} = A_2 \cos\phi_2 \\ a_{2,4} = -A_2 \sin\phi_2 \\ \cdots \end{cases} \tag{A.6}$$

then equations are as follows:

$$\begin{aligned} \mathcal{X} \times \mathcal{A} &= \mathcal{Y}, \\ \mathcal{X} \times \mathcal{A}^* &= \mathcal{Y}^*. \end{aligned} \tag{A.7}$$

Here $\mathcal{X}$ is a $[m \times n]$ matrix of equations, $\mathcal{A}$ and $\mathcal{A}^*$ are unknown one-dimensional matrices, n_t is the number of terms, and n is the number of parameters, which is twice n_t. The phase and amplitude remain constant throughout. The difference between the equations depends on the time t and the corresponding $Y(t)$. Here

$$\mathcal{X} = \begin{pmatrix} \sum_{i=1}^m X_{i,1}^2 & \sum_{i=1}^m X_{i,1}X_{i,2}\cdots & \sum_{i=1}^m X_{i,1}X_{i,n-1} & \sum_{i=1}^m X_{i,1}X_{i,n} \\ \vdots & \vdots & \vdots & \vdots \\ \sum_{i=1}^m X_{i,n}X_{i,1} & \sum_{i=1}^m X_{i,n}X_{i,2}\cdots & \sum_{i=1}^m X_{i,n}X_{i,n-1} & \sum_{i=1}^m X_{i,n}^2 \end{pmatrix},$$

$$\mathcal{A} = \begin{pmatrix} a_{1,1} \\ \vdots \\ a_{1,n} \end{pmatrix},$$

$$\mathcal{A}^* = \begin{pmatrix} a_{2,1} \\ \vdots \\ a_{2,n} \end{pmatrix},$$

$$\mathcal{Y} = \begin{pmatrix} \sum_{i=1}^m X_{2i-1,1}Y_{2i-1,t_{2i-1}} \\ \vdots \\ \sum_{i=1}^m X_{2i-1,m}Y_{t_{2i-1}} \end{pmatrix},$$

$$\mathcal{Y}^* = \begin{pmatrix} \sum_{i=1}^m X_{2i,1}Y_{t_{2i}} \\ \vdots \\ \sum_{i=1}^m X_{2i,m}Y_{t_{2i}} \end{pmatrix}.$$

For λ_6 we only use the first equation in Eq. A.7.